of the pull-down probe and actin were detected with naphthol blue black staining after immunoblot detection. The densities of RhoA in the resin eluates and the cell lysates were normalized to those of the pull-down probe and actin, respectively, and then were used to obtain the GTP-bound RhoA/total RhoA ratios.

Construction of the luciferase reporter plasmid for the human rock2 promoter assay

The promoter region of the human *rock2* gene was obtained by screening a λ Dash II human genomic library (Agilent Technology, Tokyo, Japan) with a probe obtained by PCR amplification of a 1734-bp fragment of the human *rock2* gene from human leukocyte genomic DNA. The PCR primers were designed based on the sequences in the NCBI database (Genomic contig NT_005334.15). A promoter region of the *rock2* gene in the genomic clone was then amplified by PCR and subcloned into a luciferase reporter plasmid pGL3-basic (Promega, Tokyo, Japan). The sequences of the insert were confirmed to be identical to those of the clone of the genomic library. The reporter plasmid was thus pGL3-rock2 (−1337 to +74). The number in parentheses indicates the residue numbers at the 5′ - and 3′ ends of the promoter region, respectively, while the first base of the first exon was assigned to be +1.

Luciferase assay

The cells were transfected 24 hr after the initial plating, with 2 μg pGL3-rock2 (−1337 to +74), 1 μg expression vector of clock gene (Origene, Rockville, MD, U.S.A.) and 0.5 μg phRL-TK (Promega) in 2 ml DMEM containing 10 μl lipofectamine (Invitrogen). The culture medium was replaced 6 hr after transfection, and the promoter activity was evaluated 32 hr after transfection. The clock genes examined were pCMV-XL4-REV-ERBα, pCMV-XL4-RORα, pCMV-XL5-REV-ERBβ, pCMV-XL5-RORβ, and pCMV-XL5-RORγ. The cells were washed in PBS twice, and then were lysed in passive lysis buffer (Promega). The lysates were kept frozen at −80°C until use. After thawing and clarification of the lysates by a brief centrifugation on a tabletop microcentrifuge (13,000×g, 30 sec, room temperature), the luciferase activity was determined using the dual-luciferase reporter assay system (Promega) and a Lumat LB9507 luminometer (Berthold Technologies, Bad Wildbad, Germany). The activity of firefly luciferase was normalized to that of renilla luciferase, and the value obtained with the empty vector, pCMV-XL4 or pCMV-XL5, was considered to be 1.

Tension measurement in the α-toxin-permeabilized preparations of mouse aortas

At the indicated Zeitgeber times, mice were euthanized under pentobarbital anesthesia. The ascending aorta was then immediately excided and cut into ring preparations. Next, the aortic rings were permeabilized with 5,000 units/mL staphylococcal α-toxin (Sigma, St. Louis, MO, USA) in cytosolic substitution solution (CSS) for 60 min at 30°C, as previously described.[4,6] These permeabilized preparations were then mounted between two tungsten wires and were stretched to 1.5-fold their resting length. After obtaining complete relaxation in Ca^{2+}-free CSS, the experimental protocol was started, and the tension development was recorded at 30°C. Each ring preparation was used to examine the contractile response to either a step-wise increase in the Ca^{2+} concentration, 10 μmol/L GTPγS (Sigma) or 1 μmol/L U46619 (Sigma) at each Zeitgeber time point. The response to GTPγS was examined during the precontraction induced by 0.3, 0.5 or 1 μmol/L Ca^{2+}. The response to U46619 was examined in the presence of 10 μmol/L GTP during the contraction induced by 0.5 μmol/L Ca^{2+}. The entire procedure, from euthanization to tension measurement, was completed within 1.5-2 hr. The composition of the Ca^{2+}-free CSS was 100 mmol/L potassium methanesulphonate, 2.2 mmol/L Na_2ATP, 3.38 mmol/L $MgCl_2$, 10 mmol/L EGTA, 10 mmol/L creatine phosphate, and 20 mmol/L Tris-malate (pH 6.8). CSS containing the indicated concentrations of free Ca^{2+} was prepared by adding an appropriate amount of $CaCl_2$, while assuming the Ca^{2+}-EGTA binding constant to be 10^6 L/mol.[4,6]

Trypan blue exclusion test

A standard Trypan blue exclusion test was used to evaluate the viability of the porcine coronary artery smooth muscle cells after exposure to the pharmacological inhibitors (ML-9, GF109203 and Y27632). The cells cultured in a 35-mm dish were harvested 12-min exposure to the inhibitors by a brief treatment with trypsin in 0.5 mL buffer. The cell suspensions were then immediately mixed with 0.5 mL PBS containing 3 mg/ml Trypan blue, and observed in the hemocytometer under a phase-contrast micro sope (Olympus, Tokyo, Japan). The number of trypan blue positive cells and the total cells were counted. The percentage of the trypan blue positive cells in the total cells was calculated to indicate the death rate.

Other materials

Thrombin and endothelin-1 were purchased from Sigma and the Peptide Institute (Osaka, Japan), respectively. ML-9, GF109203 and Y27632 were purchased from Calbiochem (La Jolla, CA, USA).

Data analysis

The data are expressed as the means ± SEM of the indicated number of experiments or mice. Either Steel's test or Student's *t*-test was used to determine the statistical significance of the differences among groups or between two groups, respectively, as indicated in the figure legends. A value of $P < 0.05$ was considered to be statistically significant.

Supplementary Table 1. Trypan blue exclusion test of porcine coronary artery smooth muscle cells after 12-min exposure to H_2O_2 (10 mmol/L), ML-9 (10 μmol/L), GF109203 (1 μmol/L) or Y27632 (3 μmol/L). The percentage of the trypan blue positive cells out of the total cells was calculated to indicate the death rate.

	Numbers of trypan blue positive cell	Numbers of total cell	Death rate (%)
No treatment	10	778	1.29
H_2O_2	411	452	90.9
ML-9	7	487	1.44
GF109203	5	580	0.86
Y27632	9	576	1.56

Supplementary Table 2. A comparison of the ROR response elements in the promoter region of the mammalian *rock2* genes.

species	distal element	proximal element	Numbers of nucleotide between two elements
Homo sapiens	-1028 GGTTTTGGTCA	-913 TTACTGGGTCA	104 nt
Mus musculus	-1039 GGTTTTGGTCA	-920 TTACTGGGTCA	108 nt
Rattus norvegicus	-1026 GGCTTTGGTCA	-907 TTACTGGGTCA	108 nt
Macaca mulatta	-1030 GGTTTTGGTCA	-915 TTACTGGGTCA	104 nt
Bos taurus	-470 GGTTTTGGTCA	-357 TTACTGGGTCA	102 nt
Pan troglodytes	-2496 GGTTTTGGTCA	-2381 TTACTGGGTCA	104 nt

The transcription start site is assigned +1. The residues corresponding to the consensus sequences of ROR response element [7] are highlighted in red.

Supplementary Figure 1

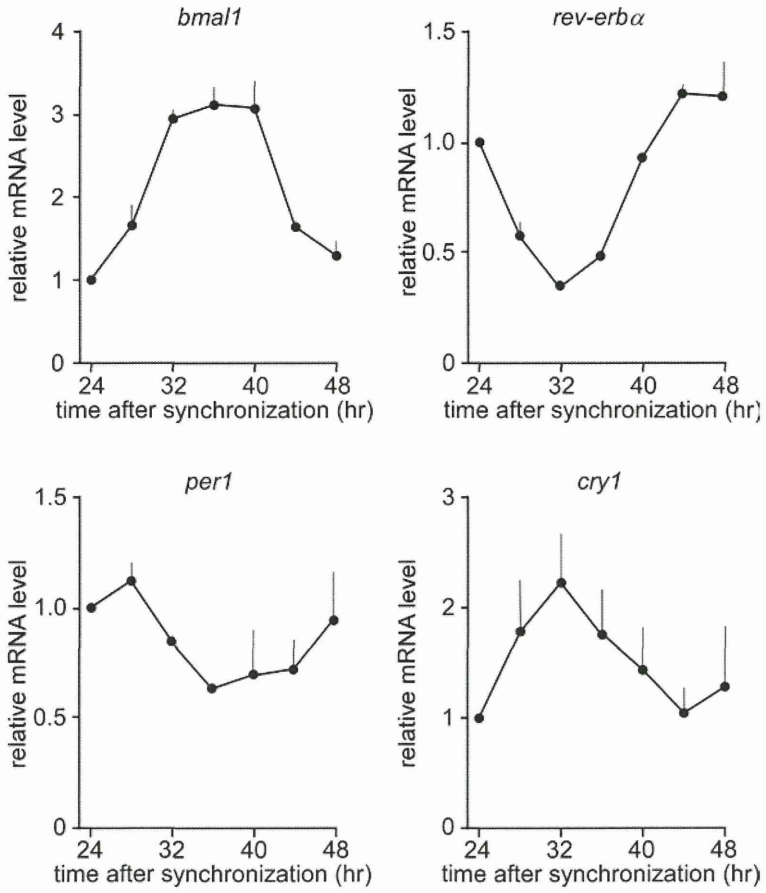

Supplementary Figure 2

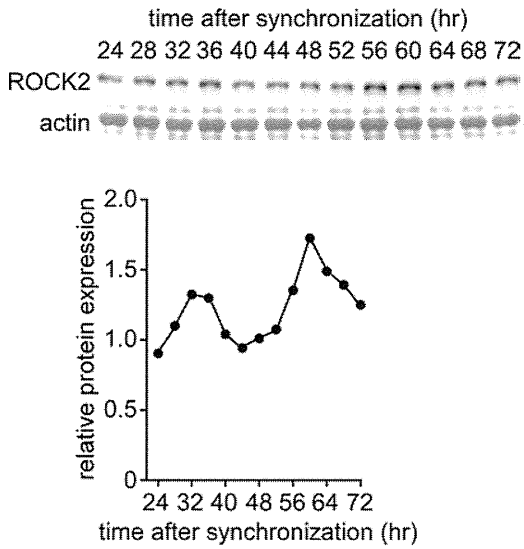

Supplementary Figure 3

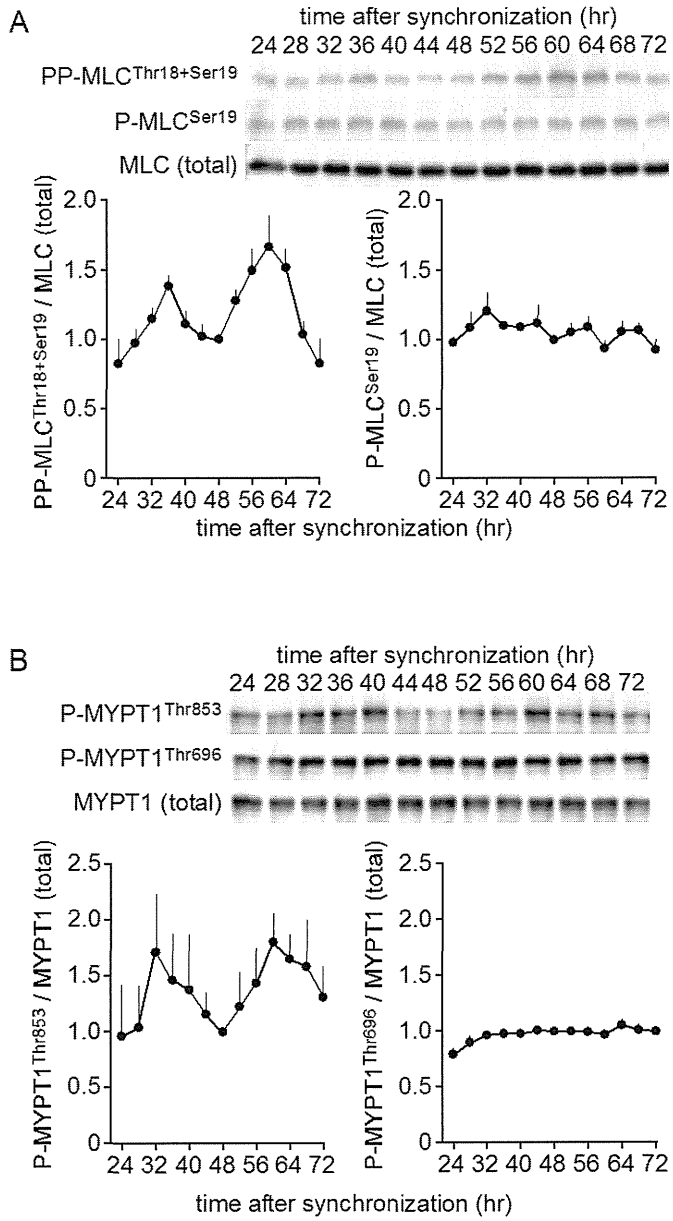

Supplementary Figure 4

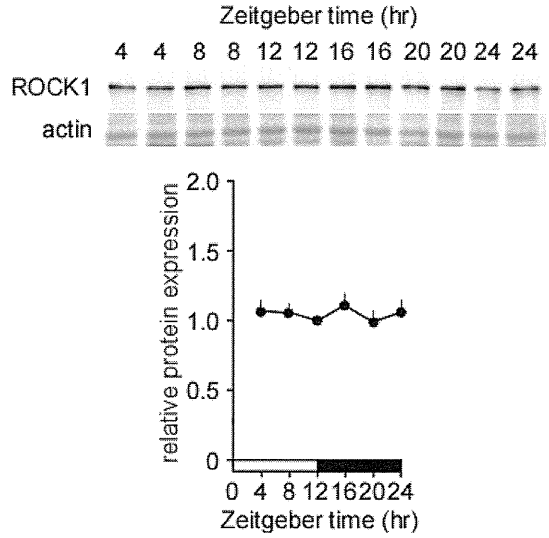

Supplementary Figure Legends

Supplementary Figure 1. The circadian changes in the expression of clock genes in porcine coronary artery smooth muscle cells.

The mRNA levels of canonical clock genes at the indicated times after synchronization of the circadian rhythm were analyzed by quantitative PCR (n=3). The levels were expressed as the relative values to those obtained at 24 hr. All data are expressed as the means ± SEM.

Supplementary Figure 2. The circadian changes in the expression of ROCK2 in porcine aortic smooth muscle cells.

The circadian changes in the level of the ROCK2 protein at the indicated times after synchronization (n=2). The data are expressed as relative values to those obtained at 48 hr.

Supplementary Figure 3. The circadian changes in the phosphorylation of myosin light chain (MLC) and MYPT1 induced by endothelin-1 in porcine coronary artery smooth muscle cells.

(A, B) The circadian changes in the phosphorylation of MLC at Thr18 and Ser19 (A; n=3), and the phosphorylation of MYPT1 at the residues corresponding to Thr696 and Thr853 in human MYPT1 (B; n=3) obtained 2 min after the stimulation with 100 nmol/L endothelin-1 at the indicated times after synchronization (n=3). The levels of phosphorylation, as normalized to the level of total MLC (A) and total MYPT1 (B), were expressed as relative values to those obtained at 48 hr. All data are expressed as the means ± SEM.

Supplementary Figure 4. The absence of a circadian rhythm in the expression of ROCK1 in the aortas of wild-type mice.

A representative immunoblot and summary showing the circadian pattern of the expression of ROCK1 protein in the aortas of wild-type mice. The mice were housed under 12-hr light (open bar) and 12-hr dark (closed bar) cycle conditions. The expression levels are expressed as the relative values to those obtained at Zeitgeber time 12. All data are expressed as the means ± SEM (n=4).

Supplementary References

1. Bi D, Nishimura J, Niiro N, Hirano K, Kanaide H. Contractile properties of the cultured vascular smooth muscle cells: the crucial role played by RhoA in the regulation of contractility. *Circ Res.* 2005;96:890-897.
2. Hamilton BA, Frankel WN, Kerrebrock AW, Hawkins TL, FitzHugh W, Kusumi K, Russell LB, Mueller KL, van Berkel V, Birren BW, Kruglyak L, Lander ES. Disruption of the nuclear hormone receptor RORα in staggerer mice. *Nature.* 1996;379:736-739.
3. Qiu CH, Shimokawa N, Iwasaki T, Parhar IS, Koibuchi N. Alteration of cerebellar neurotropin messenger ribonucleic acids and the lack of thyroid hormone receptor augmentation by staggerer-type retinoic acid receptor-related orphan receptor-α mutation. *Endocrinology.* 2007;148:1745-1753.
4. Kikkawa Y, Kameda K, Hirano M, Sasaki T, Hirano K. Impaired feedback regulation of the receptor activity and the myofilament Ca^{2+} sensitivity contributes to increased vascular reactiveness after subarachnoid hemorrhage. *J Cereb Blood Flow Metab.* 2010;30:1637-1650.
5. Hirano M, Kanaide H, Hirano K. Rac1-dependent transcriptional up-regulation of $p27^{Kip1}$ by homophilic cell-cell contact in vascular endothelial cells. *Biochim Biophys Acta.* 2007;1773:1500-1510.
6. Maeda Y, Hirano K, Kai Y, Hirano M, Suzuki SO, Sasaki T, Kanaide H. Up-regulation of proteinase-activated receptor 1 and increased contractile responses to thrombin after subarachnoid haemorrhage. *Br J Pharmacol.* 2007;152:1131-1139.
7. Harding HP, Lazar MA. The orphan receptor Rev-ErbA α activates transcription via a novel response element. *Mol Cell Biol.* 1993;13:3113-3121.

Hypertension Research (2012), 1–8

www.nature.com/hr

ORIGINAL ARTICLE

Mineralocorticoid receptors/epithelial Na^+ channels in the choroid plexus are involved in hypertensive mechanisms in stroke-prone spontaneously hypertensive rats

Masatsugu Nakano[1], Yoshitaka Hirooka[2], Ryuichi Matsukawa[1], Koji Ito[1] and Kenji Sunagawa[1]

Increase in cerebrospinal fluid (CSF) Na^+ concentration ($[Na^+]$) precedes hypertension and is a key step in the development of salt-induced hypertension. In the choroid plexus (CP), epithelial Na^+ channels (ENaCs) have an important role in Na^+ transport from the blood into the CSF. However, it remains unknown whether the mineralocorticoid receptors (MR)/ENaCs pathway in the CP of stroke-prone spontaneously hypertensive rats (SHRSP) is involved in neural mechanisms of hypertension. Therefore, we examined the role of the MR/ENaCs pathway in the CP in the development of hypertension in SHRSP associated with an increase in CSF $[Na^+]$. As a marker of MR activation, serum/glucocorticoid-inducible kinase 1 (Sgk1) expression levels in the CP were measured and found to be greater in SHRSP than in Wistar–Kyoto (WKY) rats. CSF $[Na^+]$ levels were also higher in SHRSP than in WKY rats. In SHRSP, high-salt intake (8%) increased blood pressure and urinary norepinephrine excretion compared with those in animals fed a regular salt diet (0.5%) for 2 weeks. Furthermore, the expression levels of MR, Sgk1 and ENaCs in the CP and the increase in CSF $[Na^+]$ were greater in SHRSP fed a high-salt diet than in those fed a regular salt diet. These alterations were attenuated by intracerebroventricular infusion of eplerenone (10 $\mu g\,kg^{-1}$ per day), except for α-ENaC and β-ENaC. We conclude that activation of the MR/ENaCs pathway in the CP contributes to hypertension via an increase in CSF $[Na^+]$, thereby exaggerating salt-induced hypertension with sympathetic hyperactivation in SHRSP.
Hypertension Research advance online publication, 25 October 2012; doi:10.1038/hr.2012.174

Keywords: brain; choroid plexus; epithelial sodium channels; mineralocorticoid receptor; sympathetic nervous system

INTRODUCTION

Hypertension is a major risk factor for cardiovascular diseases.[1] The percentages of essential hypertension patients who are salt sensitive have varied widely among study cohorts, ranging between 30 and 70%.[2] The appropriate therapeutic target of salt-induced hypertension has been determined to be volume overload, so that sodium restriction and diuretics are beneficial for salt-induced hypertension.[3,4] Abnormal sympathetic hyperactivity has also been detected in patients with salt-induced hypertension.[5,6] Thus, in addition to the role of kidney, the central nervous system has an important role in salt-induced hypertension.[6,7]

An increase in cerebrospinal fluid (CSF) Na^+ concentration ($[Na^+]$) is responsible for activation of the central sympathetic outflow.[8,9] High-salt intake elicits an increase in CSF $[Na^+]$ and causes sympathetic hyperactivity and hypertension in salt-sensitive model rats, such as Dahl S rats.[7,10] It has also been demonstrated that an increase in CSF $[Na^+]$ causes central aldosterone production, mineralocorticoid receptors (MR) activation and renin–angiotensin system (RAS) activation, thereby leading to sympathetic hyperactivity.[11] On the other hand, high-salt intake does not affect CSF $[Na^+]$, blood pressure (BP) or heart rate (HR) in normotensive model rats.[8] However, intracerebroventricular (ICV) infusion of Na^+-rich artificial CSF elicits MR activation in the hypothalamus, leading to increase in BP through sympathoexcitation in both salt-sensitive model rats and normotensive model rats, although the extent of sympathoexcitation is greater in salt-sensitive rats than in normotensive rats.[12,13] These observations suggest that an increase in Na^+ in the brain elicits sympathoexcitation irrespective of the presence/absence of salt-sensitive hypertension. However, it is possible that the mechanisms of Na^+ transport into the brain might be different between normotensive and hypertensive models.

The epithelium of the choroid plexus (CP) is the major site for production of CSF, which is later absorbed by arachnoid granulations.[14,15] Enhanced Na^+ uptake from the plasma to the CSF might

[1]Department of Cardiovascular Medicine, Kyushu University Graduate School of Medical Sciences, Fukuoka, Japan and [2]Department of Advanced Cardiovascular Regulation and Therapeutics, Kyushu University Graduate School of Medical Sciences, Fukuoka, Japan
Correspondence: Dr Y Hirooka, Department of Advanced Cardiovascular Regulation and Therapeutics, Kyushu University Graduate School of Medical Sciences, 3-1-1 Maidashi, Higashi-ku, Fukuoka 812-8582, Japan.
E-mail: hyoshi@cardiol.med.kyushu-u.ac.jp
Received 7 June 2012; revised 26 August 2012; accepted 29 August 2012

therefore be an important step in the initiation of salt-induced hypertension in salt-sensitive hypertensive models. Epithelial Na^+ channels (ENaCs) in the choroidal epithelia actively support Na^+ influx from the plasma and, in general, Na^+ levels in the CSF are higher than those in the plasma.[16] The ENaCs form a heteromultimeric channel that is composed of three homologous α-, β- and γ-subunits.[17] Both MR activation itself and the resulting MR-induced activation of serum/glucocorticoid-inducible kinase 1 (Sgk1) augment the expression of ENaCs in the kidney.[18] Sgk1 is a key downstream effector of MR signaling in the kidneys, inducing the early and late responses through regulation of the epithelial sodium channel activity, trafficking, and transcription.[19–21] The Sgk1 expression level also reflects MR activation, and used for this purpose because MR expression itself is not equal to MR activation.[22] However, the mechanism by which the MR/ENaCs pathway in the CP contributes to an increase in CSF $[Na^+]$ and sympathoexcitation, and leads to hypertension in hypertensive model rats, remains unclear.

Stroke-prone spontaneously hypertensive rats (SHRSP) serve as an experimental model of salt-loading-accelerated hypertension.[23,24] We hypothesized that an increase in CSF $[Na^+]$ might be involved in the development of hypertension in the absence of sodium loading, or might worsen hypertension in the presence of sodium loading in SHRSP via irregularities in the MR/ENaCs pathway in the CP. Therefore, the aim of the present study was to determine whether the MR/ENaCs pathway in the CP was altered in SHRSP and, if so, to examine whether this alteration was involved in abnormal sympathetic hyperactivity with or without sodium loading in SHRSP. For this purpose, we compared the expressions of MR, Sgk1 and ENaCs in the CP without sodium loading between SHRSP and Wistar–Kyoto (WKY) rats. Furthermore, we investigated these expressions in SHRSP fed a high-salt diet. Finally, we investigated the effect of ICV infusion of an MR blocker concomitant with high-salt loading on sympathetic activity and CSF $[Na^+]$.

METHODS

Animals

This study was reviewed and approved by the Committee on Ethics of Animal Experiments, Kyushu University Graduate School of Medical Sciences, and conducted according to the Guidelines for Animal Experiments of Kyushu University. Male WKY rats and SHRSP (260–330 g; 12–14 weeks old) were obtained from SLC Japan (Hamamatsu, Japan). They were housed in temperature- (23 ± 2°C) and light-controlled animal quarters and were provided with rat chow *ad libitum*.

Western blot analysis

Rats were killed with an overdose of sodium pentobarbital and the tissues of CP were obtained. The tissues were removed and homogenized in a lysis buffer. The protein concentration was determined using a bicinchonic acid protein assay kit (Pierce Chemical, Rockford, IL, USA). A 15-μg aliquot of protein from each sample was separated on a polyacrylamide gel with 10% sodium dodecyl sulfate. The proteins were then transferred onto polyvinylidene difluoride membranes (Immobilon-P membranes; Millipore, Billerica, MA, USA), and the membranes were incubated with rabbit immunoglobulin G (IgG) polyclonal antibody to MR (1:1000; Santa Cruz Biotechnology, Santa Cruz, CA, USA), with goat IgG polyclonal antibody to α-ENaC, rabbit polyclonal antibody to β-ENaC or rabbit polyclonal antibody to γ-ENaC (1:1000; Santa Cruz Biotechnology), or with rabbit IgG polyclonal antibody to Sgk1 (1:1000; Abcam, Cambridge, UK). Next, the membranes were incubated with horseradish peroxidase-conjugated horse anti-rabbit or anti-goat IgG antibody (1:10 000). Glyceraldehyde 3-phosphate dehydrogenase (GAPDH) was used as an internal control for the brain tissues. Immunoreactivity was detected by enhanced chemiluminescence autoradiography (ECL Western blotting detection kit; Amersham Pharmacia Biotech, Uppsala, Sweden), and the film was analyzed using the public domain software NIH Image (developed at the US National Institutes of Health and available on the Internet at http://rsb.info.nih.gov/nih-image/).

Measurement of CSF $[Na^+]$ and plasma $[Na^+]$

The CSF was collected via puncture of the cisterna magna. CSF $[Na^+]$ was measured using an ion-selective electrode (model MI-425; Microelectrodes, Bedford, NH, USA). Plasma $[Na^+]$ was measured at SRL (Tokyo, Japan).

Intracarotid artery (ICA) infusion of NaCl in acute experiments

Rats were anesthetized with pentobarbital (50 mg kg^{-1} i.p. followed by 20 mg kg^{-1} h^{-1} i.v.) and artificially ventilated. A catheter (polyethylene (PE)-50 tubing) was inserted into the left internal carotid artery and NaCl (0.5 M, 1 M, 10 s for each injection, total infusion volume; 300 μl) was administered. A catheter was implanted into the left ICA and advanced 1.0–1.3 cm beyond the carotid sinus to avoid activation of arterial baroreceptors. Another catheter was then inserted into the left femoral artery to measure BP and HR. A pair of stainless steel bipolar electrodes was placed beneath the renal nerve to record multifiber renal sympathetic nerve activity.[25,26] All signals were recorded on a computer using a PowerLab system (AD Instruments, Colorado Springs, CO, USA). The signal from the electrodes was amplified, passed through a band pass filter, and then rectified and integrated (resetting every 0.1 s).

Measurements of BP and sympathetic activity in chronic experiments

Systolic BP of conscious animals was measured using tail-cuff plethysmography (BP-98 A; Softron, Tokyo, Japan). Sympathetic activity was evaluated by measuring 24-h urinary norepinephrine excretion using high-performance liquid chromatography before and at day 14. Urinary norepinephrine excretion was calculated as described previously.[27]

ICV infusion of eplerenone

Under sodium pentobarbital anesthesia (50 mg kg^{-1} i.p.) rats were placed in a stereotaxic frame. The skin overlying the midline of the skull was incised and a small hole was made with a dental drill at the following coordinates: 0.8 mm posterior and 1.5 mm lateral relative to bregma. The infusion cannula from an Alzet brain infusion kit 2 (DURECT Corporation, Cupertino, CA, USA) connected to an osmotic pump (model 2002; Alzet) was lowered 3.5 mm below the skull surface and fixed to the skull surface with tissue adhesive. The osmotic mini pump was inserted subcutaneously in the back. The ICV infusion of artificial CSF + vehicle (1% DMSO) or artificial CSF + eplerenone (10 μg kg^{-1}per day in vehicle) (kindly provided by Pfizer Pharmaceutical Company, New York, NY, USA) for 2 weeks was performed in conjunction with feeding of a high-salt diet, and the infusion and diet were started simultaneously.

Experimental protocols

Protocol 1: Experiments with rats without salt loading. (1) Western blot analysis of MR, Sgk1 and ENaCs in the CP of SHRSP and WKY rats; (2) evaluations of CSF $[Na^+]$ and plasma $[Na^+]$ in SHRSP and WKY rats; (3) acute bolus ICA injection of NaCl (0.5 M, 1 M, 300 μl per 10 s) in SHRSP and WKY rats. The rats were fed a regular diet.

Protocol 2: Experiments with rats fed a high-salt diet. SHRSP and WKY rats were divided randomly into two groups: rats fed a high-salt (8% NaCl) diet for 2 weeks and rats fed a regular (0.5% NaCl) diet for 2 weeks. Then, the following protocols were performed. (1) Western blot analysis of MR, Sgk1 and ENaCs in the CP of SHRSP and WKY rats fed a high-salt or regular diet; (2) evaluations of CSF $[Na^+]$ in SHRSP and WKY rats fed a high-salt diet.

Protocol 3: Experiments with SHRSP fed a high-salt diet with eplerenone. ICV infusion of artificial CSF or eplerenone for 2 weeks in SHRSP fed a high-salt diet. Then, the following protocols were performed. (1) Measurement of BP and HR using the tail-cuff method; (2) western blot analysis of MR, Sgk1 and

ENaCs in the CP; (3) Evaluations of CSF [Na^+] and urinary norepinephrine in SHRSP.

Statistical analysis

All values are expressed as the means ± s.e.m. Intergroup differences in the mean arterial pressure (MAP) and HR values obtained using the PowerLab and tail-cuff method were compared using two-way analysis of variance. In the analysis of variance, comparisons between any two mean values were performed using Bonferroni's correction for multiple comparisons. The MR, Sgk1 and ENaCs protein expression values (western blot analysis), and the CSF [Na^+] and plasma [Na^+] values were compared using an unpaired *t*-test. Values of $P<0.05$ were considered statistically significant.

RESULTS

Baseline MR, Sgk1 and ENaCs expressions in the CP of SHRSP and WKY rats fed a regular diet

MR expression in SHRSP did not differ from that in WKY rats, while Sgk1 expression was significantly greater in SHRSP (Figure 1a). The expressions of α-ENaC, β-ENaC and γ-ENaC were also significantly higher in SHRSP than in WKY rats (Figure 1b).

Baseline plasma [Na^+] and CSF [Na^+] of SHRSP and WKY rats fed a regular diet

Plasma [Na^+] levels did not differ between WKY rats and SHRSP (WKY, 145.4 ± 0.8 mM; SHRSP, 145.1 ± 0.8 mM; $n=7$ for each), but the level of CSF [Na^+] was greater in SHRSP (WKY, 151.9 ± 0.4 mM; SHRSP, 155.5 ± 0.3 mM, $n=6$ for each; Figure 1c).

Effect of ICA NaCl infusion on MAP, HR and renal sympathetic nerve activity in SHRSP and WKY rats

ICA hypertonic NaCl (0.5 M, 1.0 M) infusions increased MAP in both WKY rats and SHRSP dose-dependently. However, the degrees of increase in MAP were greater in SHRSP than in WKY rats (% change of ΔMAP: WKY *vs.* SHRSP, 3.0 ± 2.3% *vs.* 14.4 ± 2.5%, $P<0.05$ (0.5 M); 7.5 ± 4.3% *vs.* 35.1 ± 5.5%, $P<0.005$ (1.0 M); $n=5$ for each; Figure 2). The duration of the responses lasted longer in SHRSP than WKY rats (WKY *vs.* SHRSP, 2.3 ± 0.4 *vs.* 5.9 ± 0.6 min, $P<0.01$ (0.5 M); 4.3 ± 0.5 *vs.* 14.3 ± 1.5 min, $P<0.01$ (1.0 M); $n=5$ for each). Peak responses of renal sympathetic nerve activity (% baseline) to NaCl were also greater in SHRSP than in WKY rats (% baseline: WKY *vs.* SHRSP, 6.5 ± 3.7% *vs.* 20.3 ± 1.1%, $P<0.01$ (0.5 M); 13.8 ± 1.7% *vs.* 30.0 ± 5.3%, $P<0.05$ (1.0 M); $n=4$-5 for each; Figure 2).

Effects of high-salt diet on systolic BP and CSF [Na^+] in SHRSP and WKY rats

Systolic BP and HR of in SHRSP groups were significantly higher than those of WKY rats throughout the study (Table 1). SHRSP fed a high-salt diet exhibited a significantly higher systolic BP and HR than SHRSP fed a regular diet, starting at 12 weeks of age ($P<0.05$). Systolic BP also slightly increased in SHRSP fed a regular diet ($P<0.05$). Systolic BP and HR values for 2 weeks are shown in

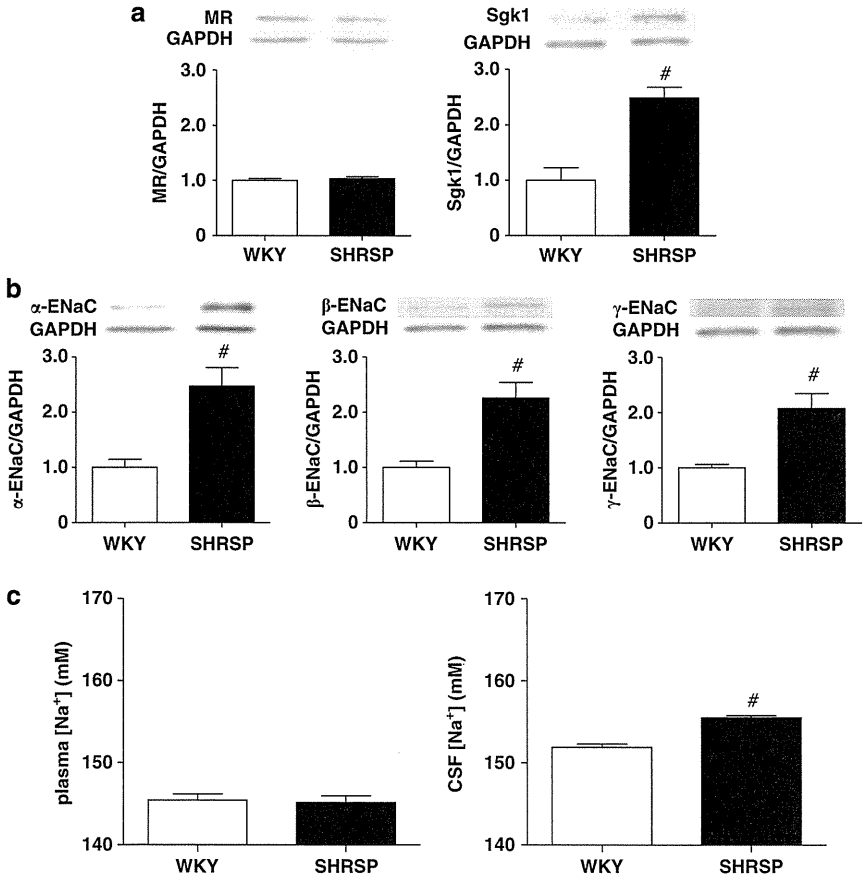

Figure 1 Western blot analysis demonstrating the expression levels of (**a**) the MR and Sgk1, and (**b**) α-, β- and γ-ENaCs in the CP of 12-week-old WKY and SHRSP rats. The densitometric average was normalized to the values obtained from the analysis of glyceraldehyde-3-phosphatase dehydrogenase (GAPDH) as an internal control. Expressions are shown relative to those seen in WKY rats, which are assigned a value of 1. Values are expressed as the mean ± s.e.m. $^{\#}P<0.01$; $n=4$–5. (**c**) Plasma [Na^+] and CSF [Na^+] levels in WKY rats and SHRSP. $^{\#}P<0.01$; $n=6$–7.

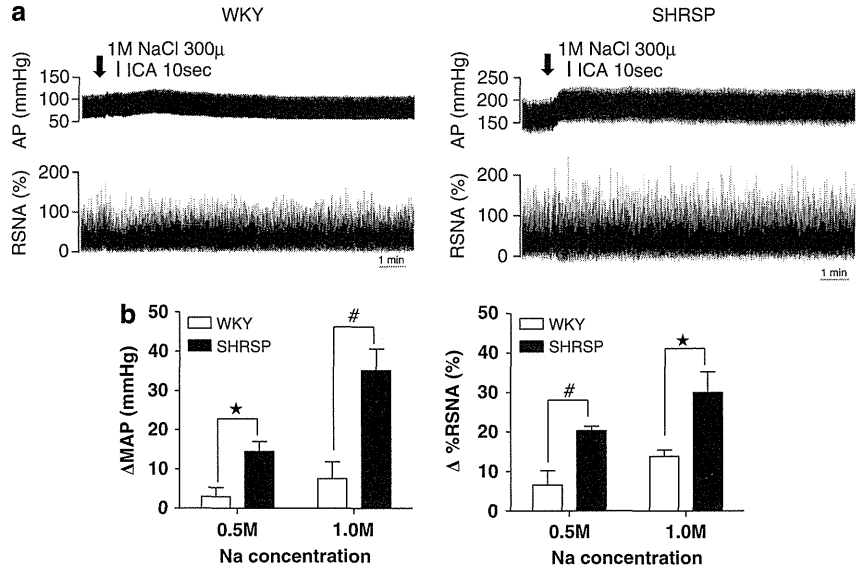

Figure 2 The responses of arterial pressure (AP) and renal sympathetic nerve activity (RSNA) to ICA NaCl (0.5 M, 1 M) infusions. (**a**) Raw data of the changes in AP and RSNA after ICA NaCl (1 M) infusions in WKY rats and SHRSP. (**b**) Group data of the changes in MAP and RSNA in response to ICA NaCl (0.5 M, 1 M) infusions. Values are expressed as the mean ± s.e.m. $^{*}P<0.05$, $^{\#}P<0.01$; $n=4$–5.

Table 1 BP and HR with a regular diet or a high-salt diet in WKY and SHRSP

	Systolic BP (mm Hg)				*HR (b.p.m.)*			
Weeks	*HS-SP*	*RS-SP*	*HS-W*	*RS-W*	*HS-SP*	*RS-SP*	*HS-W*	*RS-W*
12	219 ± 3$^{\#}$	216 ± 2$^{\#}$	134 ± 2	135 ± 2	374 ± 2$^{\#}$	373 ± 3$^{\#}$	352 ± 2	349 ± 4
13	235 ± 4$^{\#*}$	223 ± 2$^{\#}$	137 ± 2	134 ± 2	385 ± 4$^{\#*}$	373 ± 4$^{\#}$	359 ± 5	356 ± 3
14	253 ± 2$^{\#*}$	227 ± 2$^{\#}$	138 ± 2	136 ± 1	390 ± 2$^{\#*}$	370 ± 4$^{\#}$	358 ± 3	351 ± 5

Abbreviations: BP, blood pressure; HR, heart rate; HS-SP, high-salt diet SHRSP rats; HS-W, high-salt diet WKY rats; RS-SP, regular diet SHRSP rats; RS-W, regular diet WKY rats; SHRSP, spontaneously hypertensive stroke-prone rats; WKY, Wistar–Kyoto rats.
Values are given as mean ± s.e.m. $^{*}P<0.05$, HS-SP *vs.* RS-SP; $^{\#}P<0.05$, SHRSP *vs.* WKY. $n=7$.

Table 1. CSF [Na^+] in SHRSP also started to increase from day 4 (152.3 ± 0.8 *vs.*158.6 ± 0.4 mM, $P<0.05$). At day 14, CSF [Na^+] in SHRSP fed a high-salt diet was significantly greater than in WKY fed a high-salt diet (152.4 ± 0.4 *vs.*161.1 ± 0.4 mM; Figure 3a). In contrast, in WKY rats, there were no significant changes in systolic BP and CSF [Na^+] during the observation (Figure 3a and Table 1).

Expression of MR, Sgk1 and ENaCs in the CP in SHRSP and WKY rats fed a high-salt diet

The expressions of MR, Sgk1 and ENaCs were significantly greater in SHRSP fed a high-salt diet than in those fed a regular diet (Figure 3b). The expressions of MR, Sgk1 and ENaCs were similar between WKY rats fed a high-salt diet and those fed a regular diet (Figure 3c).

Effects of eplerenone on systolic BP, sympathetic activity, CSF [Na^+], and expression levels of MR, Sgk1 and ENaCs in SHRSP fed a high-salt diet

ICV infusion of eplerenone attenuated the increases in urinary norepinephrine and systolic BP in SHRSP fed a high-salt diet (Figures 4a and b). ICV infusion of eplerenone attenuated the increase in CSF [Na^+] in SHRSP fed a high-salt diet (157.8 ± 0.92 *vs.* 161.0 ± 0.73 mM; Figure 4c). ICV infusion of eplerenone did not attenuate the enhanced expressions of MR, α-ENaC and β-ENaC, but did attenuate Sgk1 and γ-ENaC expression (Figures 5a and b).

DISCUSSION

The present study demonstrated that the MR/ENaCs pathway in the CP of SHRSP was activated before salt loading, leading to an increase in the CSF [Na^+] and eliciting sympathetic hyperactivity. Salt loading then elicited further activation of this pathway in the CP and an additional increase in CSF [Na^+], thereby causing further sympathetic hyperactivity and BP elevation.

We first investigated the alterations of the Na^+ transport system in the CP of SHRSP and found that the expressions of all subunit types of ENaCs were greater in SHRSP than in WKY rats. These data suggest that the function of the Na^+ transport system in the CP was enhanced in SHRSP. In fact, the plasma [Na^+] level was similar between SHRSP and WKY rats, but the CSF [Na^+] level was greater in SHRSP than in WKY rats. Taken together, these data suggest that activation of ENaCs in the CP elicited increase in CSF [Na^+] in SHRSP.

We considered that these alterations occurring in SHRSP may contribute to the development of hypertension. Thus, we investigated whether activated ENaCs in the CP contribute to the development of hypertension with sympathetic hyperactivity. ICA infusions of hypertonic NaCl solutions increased renal sympathetic nerve activity and AP and the degrees of these changes were greater in SHRSP than in WKY rats. It has been reported that increases in the amount of plasma [Na^+] perfusing the forebrain evoke a prompt increase

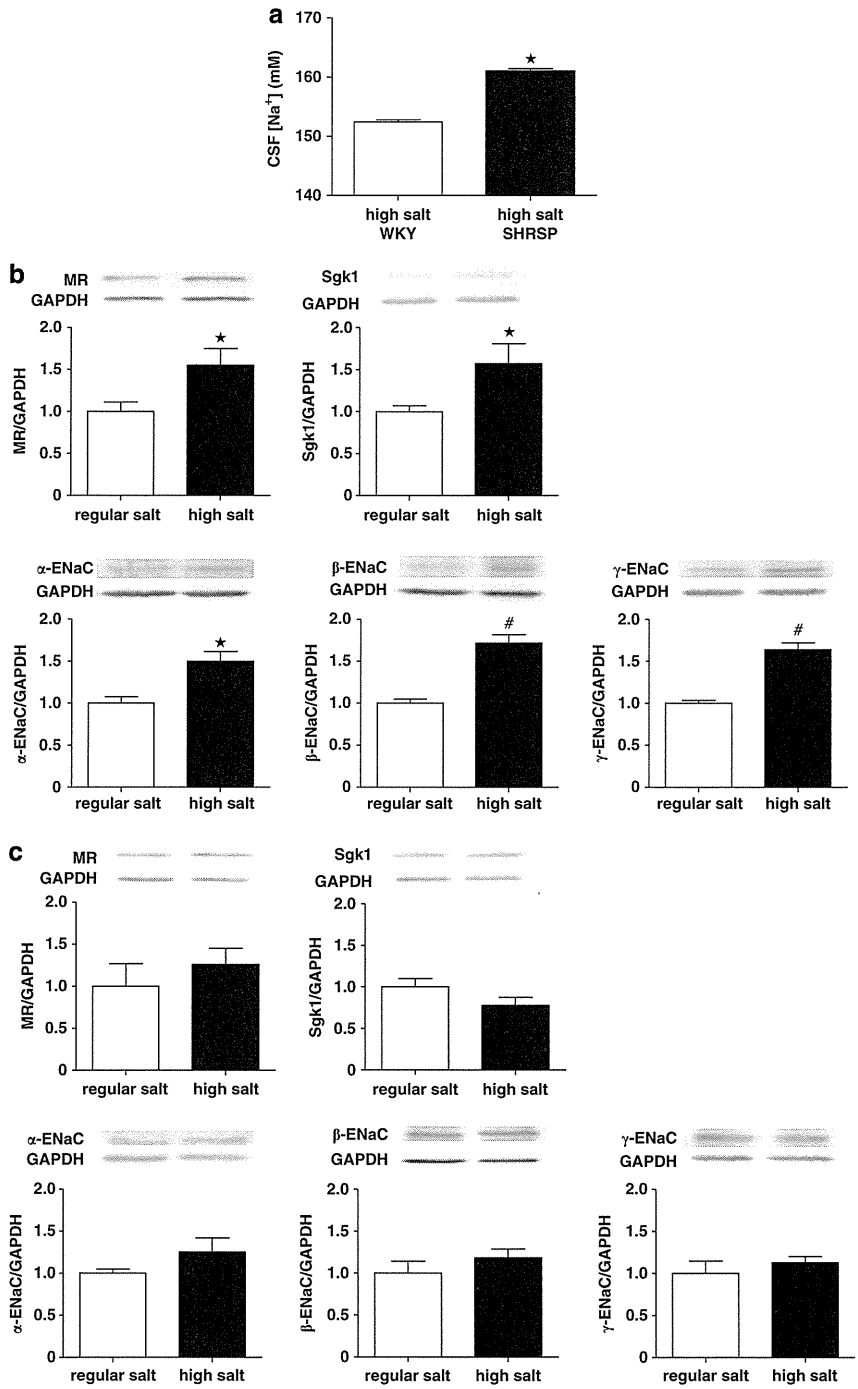

Figure 3 (**a**) CSF [Na^+] in WKY rats and SHRSP by feeding with a high-salt diet at day 14. Values are expressed as the mean ± s.e.m. $^*P<0.05$; $n=7$ for each. (**b**) Western blot analysis demonstrating MR, Sgk1, α-, β- and γ- ENaC expression in the CP in SHRSP fed a high-salt or regular diet. The densitometric average is normalized to the values obtained from the analysis of GAPDH as an internal control. Expressions are shown relative to those in SHRSP fed a regular diet, which are assigned a value of 1. (**c**) Western blot analysis demonstrating MR, Sgk1, α-, β- and γ- ENaC expression in the CP in WKY rats fed a high-salt or regular diet. The densitometric average is normalized to the values obtained from the analysis of GAPDH as an internal control. Expressions are shown relative to those in WKY rats fed a regular diet, which are assigned a value of 1. Values are expressed as the mean ± s.e.m. $^*P<0.05$, $^{\#}P<0.01$; $n=4$–6.

of sympathetic nerve activity.[28,29] An increase in CSF [Na^+] may excite Na^+-sensitive neurons in the circumventricular organs, such as the subfornical organ.[30] This increased neuronal activity could be relayed to the paraventricular nucleus of the hypothalamus or rostral ventrolateral medulla, thereby increasing sympathetic nerve activity and BP.[31–33] Furthermore, an increase in CSF [Na^+] would increase the level of hypothalamic tissue [Na^+][34] and could thereby enhance the firing activity of Na^+-sensitive neurons in the paraventricular nucleus.[35] We also need to consider the possibility that circumventricular organs could sense hyperosmolality after ICA infusions of hypertonic NaCl solutions thereby activates sympathetic activity, although there is a clear difference between SHRSP and WKY rats.[36] In addition, the duration of the responses lasted longer in SHRSP than WKY rats. We were not able to measure CSF [Na^+]

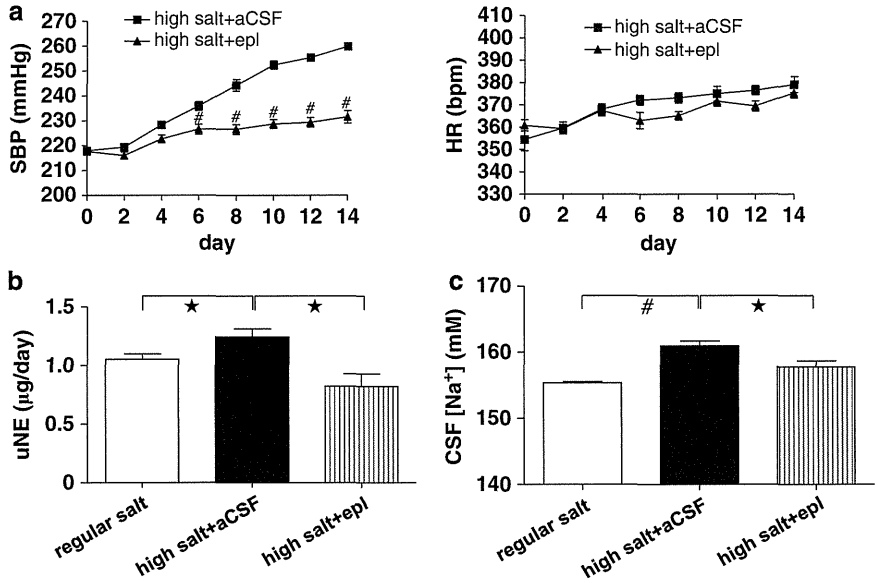

Figure 4 Effects of ICV infusion of artificial CSF (aCSF) (high salt + aCSF) *vs.* eplerenone at 10 μg kg^{-1} per day (high salt + epl) in CP of SHRSP on systolic BP (SBP), heart rate (HR), sympathetic nerve activity and CSF [Na^+] induced by high-salt intake. (**a**) Changes in resting SBP and HR response to ICV infusion of aCSF or eplerenone in rats fed a high-salt diet. $^{\#}P<0.01$; $n=6$ for each. (**b**) Group data for urinary norepinephrine excretion in SHRSP given a regular diet, a high-salt diet plus ICV infusion of aCSF (high salt + aCSF) or a high-salt diet plus eplerenone (high salt + epl). $^{*}P<0.05$; $n=5$–6. (**c**) Group data for CSF [Na^+] in SHRSP given a regular diet (regular), a high-salt diet plus ICV infusion of aCSF (high salt + aCSF) or a high-salt diet plus eplerenone (high salt + epl). $^{*}P<0.05$, $^{\#}P<0.01$; $n=10$ for each.

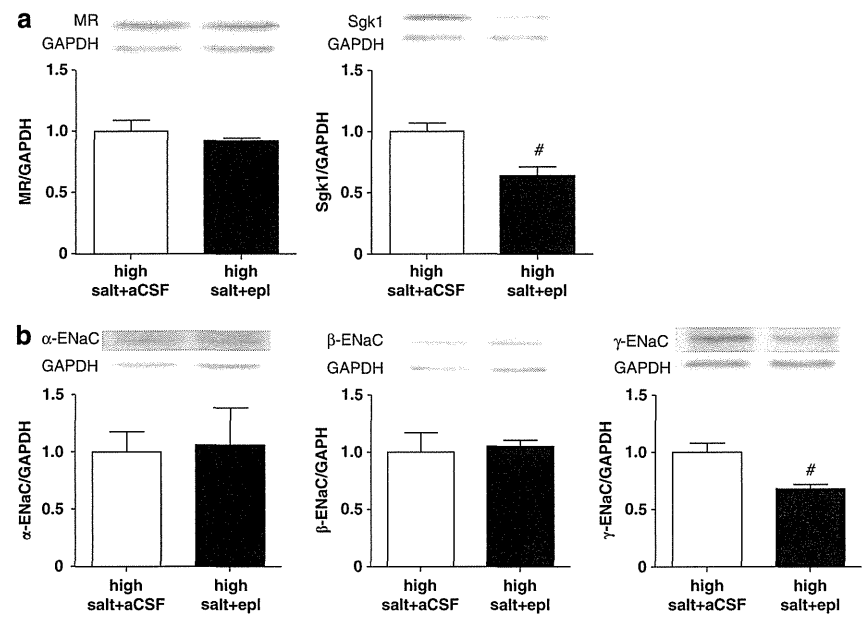

Figure 5 Effects of ICV infusion of artificial CSF (aCSF) (high salt + aCSF) *vs.* eplerenone at 10 μg kg^{-1} per day (high salt + epl) in the CP of SHRSP. Western blot analysis demonstrating the expression of (**a**) MR, Sgk1, or (**b**) α-, β- and γ- ENaC in the CP in high salt + aCSF *vs.* high salt + epl. The densitometric average was normalized to the values obtained from the analysis of glyceraldehyde-3-phosphatase dehydrogenase (GAPDH) as an internal control. Expressions are shown relative to those seen in the high salt + aCSF group, which were assigned a value of 1. Values are expressed as the mean ± s.e.m. $^{\#}P<0.01$; $n=4$–6.

before and after ICA infusion because of technical difficulties. However, these data indirectly suggest that Na^+ uptake into the CSF is enhanced and this contributes to hypertension with sympathoexcitation in SHRSP without salt loading.

In salt-sensitive model rats, high-salt intake causes an increase in CSF [Na^+] and leads to sympathetic hyperactivity and hypertension.[7,37,38] SHRSP are also known as a salt-induced hypertension model.[24] A high-salt diet elicited hypertension with sympathetic hyperactivity in SHRSP as previously described.[24,39] We found that the expressions of all subtypes of ENaCs in the CP and CSF [Na^+] were increased in SHRSP fed a high-salt diet concomitant with changes in MAP. These data suggest that activated ENaCs in the

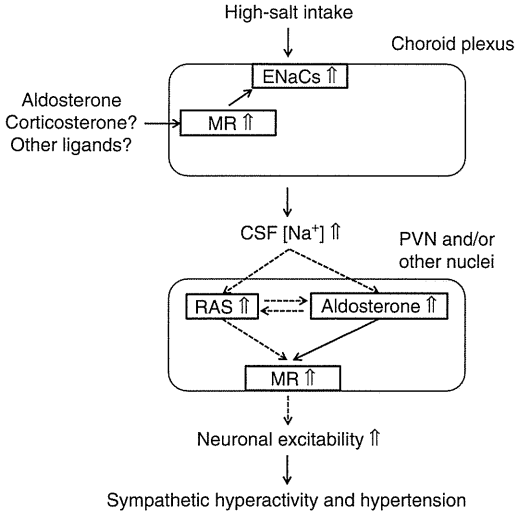

Figure 6 The possible cascade that Na^+ transport mechanisms in the central nervous system contributing to sympathetic hyperactivity and hypertension in SHRSP on high-salt intake. In SHRSP on high-salt intake, Na^+ transport into CSF is enhanced and CSF [Na^+] is increased. Activation of MR/ENaCs pathway in the choroid plexus is involved in Na^+ transport from the blood into the CSF in SHRSP. The increased CSF [Na^+] increased the neuronal activity in the PVN or other autonomic nuclei, thereby increasing the central sympathetic outflow. This, in turn, leads to sympathetic hyperactivity and hypertension. The broken lines indicate hypothetical mechanisms suggested by other investigators. RAS indicates renin–angiotensin system.

CP of SHRSP accelerated the increase in CSF [Na^+], and this increase further enhanced the levels of ENaCs, leading to sympathetic hyperactivity (Figure 6).

It has been shown that aldosterone binds to MR and increases expression and activity of ENaCs in the distal nephron of the kidney, resulting in enhanced Na^+ and water reabsorption, and presumably thereby elevated BP.[18] We recently reported that activation of the MR/ENaCs pathway is considered to be an initial step in the acquisition of Na^+ sensitivity in the brain in a pressure overload model.[40] In fact, Western blotting in the present study revealed that the expression of Sgk1 was increased in SHRSP compared with WKY rats before salt loading, although the expression levels of MR did not differ between SHRSP and WKY rats. Moreover, expressions of MR and ENaCs in the CP were increased by salt loading in SHRSP. Taken together with the alterations of ENaCs, our findings suggest that MR and ENaCs in the CP are altered in parallel with or without salt loading in SHRSP. We also found that ICV infusion of an MR blocker attenuated BP elevation and increase in CSF [Na^+] induced by chronic salt loading in SHRSP. Furthermore, the MR blocker inhibited the increase in Sgk1 expressions and γ-ENaC in the CP of SHRSP. However, we do not have a clear explanation why only γ-ENaC was smaller for eplerenon treated SHRSP on high-salt diet at the present time. There may be subunit-type-specific regulation of ENaC.[40] These findings suggest that MR regulates Na^+ transport into the CSF by regulating the expressions of ENaCs in the CP of SHRSP, although we did not find the increased expression levels of α-ENaC and β-ENaC.

In consistent with the results of a previous study, SHRSP have significantly higher plasma aldosterone levels compared with WKY rats, indicating upregulation of the aldosterone system in SHRSP.[24] If the aldosterone is the ligand of MR in the CP of SHRSP, MR is activated in SHRSP. In salt-sensitive model rats, high-salt intake produces aldosterone locally in the hypothalamus.[11,41] Another possibility is that locally produced aldosterone may affect MR activation in the CP via CSF.[41,42] In the absence of 11β-hydroxysteroid dehydrogenase type 2 in the CP, corticosterone is also a ligand for MR.[43] On the other hand, Rac1 enhances MR independent of aldosterone in the kidney.[44] We did not address precise mechanisms how MR in the CP was activated in SHRSP in the present study. Nevertheless, our findings suggest that MR activation has an important role for the increase in central sympathetic outflow in SHRSP. Further studies are necessary to clarify this important question.

The present study has some additional limitations. First, ENaCs exist on both the apical and basolateral side of the CP.[34,45] We did not examine the distribution of ENaCs in the CP in the present study because of the technical difficulty. Second, ICV infusion of an MR blocker may act on the nuclei other than those in the CP.[46,47] Third, Na^+-K^+-ATPase activity in the CP is also dependent on CSF [Na^+] in Dahl salt-sensitive rats.[48] MR regulates the transcription of Na^+-K^+-ATPase.[49] Both ENaCs and Na^+-K^+-ATPase regulate Na^+ transport in the CP. Further studies will be needed to clarify whether Na^+-K^+-ATPase alterations are involved in our observations in the present study.

In conclusion, our findings suggest that the MR/ENaCs pathway in the CP of SHRSP is activated before salt loading, leading to an increased CSF [Na^+] and eliciting sympathetic hyperactivity. Second suggestion is that salt loading elicited further activation of this pathway in the CP and additional enhancement of the CSF [Na^+] levels, leading to further sympathetic hyperactivity.

CONFLICT OF INTEREST

The authors declare no conflict of interest.

ACKNOWLEDGEMENTS

We express our sincere thanks to Naomi Shirouzu for help with the western blot analysis. This study was supported by the Grants-in-Aid for Scientific Research from the Japan Society for Promotion of Science (23220013, 24390198) and, in part, a Grant from the Salt Science Research Foundation (1233).

1 Rosamond W, Flegal K, Friday G, Furie K, Go A, Greenlund K, Haase N, Ho M, Howard V, Kissela B, Kittner S, Lloyd-Jones D, McDermott M, Meigs J, Moy C, Nichol G, O'Donnell CJ, Roger V, Rumsfeld J, Sorlie P, Steinberger J, Thom T, Wasserthiel-Smoller S, Hong Y. American Heart Association Statistics Committee and Stroke Statistics Subcommittee. Heart disease and stroke statistics–2007 update: A report from the american heart association statistics committee and stroke statistics subcommittee. *Circulation* 2007; **115**: e69–e171.
2 Rassler B. The renin-angiotensin system in the development of salt-sensitive hypertension in animal models and humans. *Pharmaceuticals* 2010; **3**: 940–960.
3 Kawano Y. Diurnal blood pressure variation and related behavioral factors. *Hypertens Res* 2011; **34**: 281–285.
4 Sica DA, Carter B, Cushman W, Hamm L. Thiazide and loop diuretics. *J Clin Hypertens* 2011; **13**: 639–643.
5 Kawano Y, Yoshida K, Kawamura M, Yoshimi H, Ashida T, Abe H, Imanishi M, Kimura G, Kojima S, Kuramochi M. Sodium and noradrenaline in cerebrospinal fluid and blood in salt-sensitive and non-salt-sensitive essential hypertension. *Clin Exp Pharmacol Physiol* 1992; **19**: 235–241.
6 Adrogue HJ, Madias NE. Sodium and potassium in the pathogenesis of hypertension. *N Engl J Med* 2007; **356**: 1966–1978.
7 Huang BS, Amin MS, Leenen FH. The central role of the brain in salt-sensitive hypertension. *Curr Opin Cardiol* 2006; **21**: 295–304.
8 Huang BS, Van Vliet BN, Leenen FH. Increases in CSF [Na^+] precede the increases in blood pressure in dahl S rats and SHR on a high-salt diet. *Am J Physiol Heart Circ Physiol* 2004; **287**: H1160–H1166.
9 Takahashi H, Yoshika M, Komiyama Y, Nishimura M. The central mechanism underlying hypertension: a review of the roles of sodium ions, epithelial sodium channels, the renin-angiotensin-aldosterone system, oxidative stress and endogenous digitalis in the brain. *Hypertens Res* 2011; **34**: 1147–1160.

10 Fujita M, Ando K, Nagae A, Fujita T. Sympathoexcitation by oxidative stress in the brain mediates arterial pressure elevation in salt-sensitive hypertension. *Hypertension* 2007; **50**: 360–367.
11 Huang BS, White RA, Jeng AY, Leenen FH. Role of central nervous system aldosterone synthase and mineralocorticoid receptors in salt-induced hypertension in dahl salt-sensitive rats. *Am J Physiol Regul Integr Comp Physiol* 2009; **296**: R994–R1000.
12 Huang BS, Wang H, Leenen FH. Enhanced sympathoexcitatory and pressor responses to central Na^+ in dahl salt-sensitive vs. -resistant rats. *Am J Physiol Heart Circ Physiol* 2001; **281**: H1881–H1889.
13 Huang BS, White RA, Ahmad M, Jeng AY, Leenen FH. Central infusion of aldosterone synthase inhibitor prevents sympathetic hyperactivity and hypertension by central Na^+ in wistar rats. *Am J Physiol Regul Integr Comp Physiol* 2008; **295**: R166–R172.
14 Praetorius J. Water and solute secretion by the choroid plexus. *Pflugers Arch* 2007; **454**: 1–18.
15 Brown PD, Davies SL, Speake T, Millar ID. Molecular mechanisms of cerebrospinal fluid production. *Neuroscience* 2004; **129**: 957–970.
16 Amin MS, Wang HW, Reza E, Whitman SC, Tuana BS, Leenen FH. Distribution of epithelial sodium channels and mineralocorticoid receptors in cardiovascular regulatory centers in rat brain. *Am J Physiol Regul Integr Comp Physiol* 2005; **289**: R1787–R1797.
17 Canessa CM, Schild L, Buell G, Thorens B, Gautschi I, Horisberger JD, Rossier BC. Amiloride-sensitive epithelial Na^+ channel is made of three homologous subunits. *Nature* 1994; **367**: 463–467.
18 Schild L. The epithelial sodium channel and the control of sodium balance. *Biochim Biophys Acta* 2010; **1802**: 1159–1165.
19 Wulff P, Vallon V, Huang DY, Volkl H, Yu F, Richter K, Jansen M, Schlunz M, Klingel K, Loffing J, Kauselmann G, Bosl MR, Lang F, Kuhl D. Impaired renal Na^+ retention in the sgk1-knockout mouse. *J Clin Invest* 2002; **110**: 1263–1268.
20 Pearce D, Kleyman TR. Salt, sodium channels, and SGK1. *J Clin Invest* 2007; **117**: 592–595.
21 Zhang W, Xia X, Reisenauer MR, Rieg T, Lang F, Kuhl D, Vallon V, Kone BC. Aldosterone-induced Sgk1 relieves Dot1a-Af9-mediated transcriptional repression of epithelial na+ channel alpha. *J Clin Invest* 2007; **117**: 773–783.
22 Quinkler M, Zehnder D, Eardley KS, Lepenies J, Howie AJ, Hughes SV, Cockwell P, Hewison M, Stewart PM. Increased expression of mineralocorticoid effector mechanisms in kidney biopsies of patients with heavy proteinuria. *Circulation* 2005; **112**: 1435–1443.
23 Camargo MJ, von Lutterotti N, Campbell Jr WG, Pecker MS, James GD, Timmermans PB, Laragh JH. Control of blood pressure and end-organ damage in maturing salt-loaded stroke-prone spontaneously hypertensive rats by oral angiotensin II receptor blockade. *J Hypertens* 1993; **11**: 31–40.
24 Endemann DH, Touyz RM, Iglarz M, Savoia C, Schiffrin EL. Eplerenone prevents salt-induced vascular remodeling and cardiac fibrosis in stroke-prone spontaneously hypertensive rats. *Hypertension* 2004; **43**: 1252–1257.
25 Nishihara M, Hirooka Y, Matsukawa R, Kishi T, Sunagawa K. Oxidative stress in the rostral ventrolateral medulla modulates excitatory and inhibitory inputs in spontaneously hypertensive rats. *J Hypertens* 2012; **30**: 97–106.
26 Matsukawa R, Hirooka Y, Nishihara M, Ito K, Sunagawa K. Neuregulin-1/ErbB signaling in rostral ventrolateral medulla is involved in blood pressure regulation as an antihypertensive system. *J Hypertens* 2011; **29**: 1735–1742.
27 Ito K, Kimura Y, Hirooka Y, Sagara Y, Sunagawa K. Activation of rho-kinase in the brainstem enhances sympathetic drive in mice with heart failure. *Auton Neurosci* 2008; **142**: 77–81.
28 Schad H, Seller H. Influence of intracranial osmotic stimuli on renal nerve activity in anaesthetized cats. *Pflugers Arch* 1975; **353**: 107–121.
29 Kumagai H, Oshima N, Matsuura T, Iigaya K, Imai M, Onimaru H, Sakata K, Osaka M, Onami T, Takimoto C, Kamayachi T, Itoh H, Saruta T. Importance of rostral ventrolateral medulla neurons in determining efferent sympathetic nerve activity and blood pressure. *Hypertens Res* 2012; **35**: 132–141.
30 Denton DA, McKinley MJ, Weisinger RS. Hypothalamic integration of body fluid regulation. *Proc Natl Acad Sci USA* 1996; **93**: 7397–7404.
31 Cato MJ, Toney GM. Angiotensin II excites paraventricular nucleus neurons that innervate the rostral ventrolateral medulla: An *in vitro* patch-clamp study in brain slices. *J Neurophysiol* 2005; **93**: 403–413.
32 Li DP, Chen SR, Pan HL. Angiotensin II stimulates spinally projecting paraventricular neurons through presynaptic disinhibition. *J Neurosci* 2003; **23**: 5041–5049.
33 Hirooka Y. Oxidative stress in the cardiovascular center has a pivotal role in the sympathetic activation in hypertension. *Hypertens Res* 2011; **34**: 407–412.
34 Wang HW, Amin MS, El-Shahat E, Huang BS, Tuana BS, Leenen FH. Effects of central sodium on epithelial sodium channels in rat brain. *Am J Physiol Regul Integr Comp Physiol* 2010; **299**: R222–R233.
35 Gabor A, Leenen FH. Mechanisms in the PVN mediating local and central sodium-induced hypertension in wistar rats. *Am J Physiol Regul Integr Comp Physiol* 2009; **296**: R618–R630.
36 Shi P, Martinez MA, Calderon AS, Chen Q, Cunningham JT, Toney GM. Intra-carotid hyperosmotic stimulation increases fos staining in forebrain organum vasculosum laminae terminalis neurones that project to the hypothalamic paraventricular nucleus. *J Physiol* 2008; **586**: 5231–5245.
37 Suzuki J, Ogawa M, Tamura N, Maejima Y, Takayama K, Maemura K, Honda K, Hirata Y, Nagai R, Isobe M. A critical role of sympathetic nerve regulation for the treatment of impaired daily rhythm in hypertensive Dahl rats. *Hypertens Res* 2010; **33**: 1060–1065.
38 Brooks VL, Haywood JR, Johnson AK. Translation of salt retention to central activation of the sympathetic nervous system in hypertension. *Clin Exp Pharmacol Physiol* 2005; **32**: 426–432.
39 Koga Y, Hirooka Y, Araki S, Nozoe M, Kishi T, Sunagawa K. High salt intake enhances blood pressure increase during development of hypertension via oxidative stress in rostral ventrolateral medulla of spontaneously hypertensive rats. *Hypertens Res* 2008; **31**: 2075–2083.
40 Ito K, Hirooka Y, Sunagawa K. Blockade of mineralocorticoid receptors improves salt-induced left-ventricular systolic dysfunction through attenuation of enhanced sympathetic drive in mice with pressure overload. *J Hypertens* 2010; **28**: 1449–1458.
41 Gomez-Sanchez EP, Ahmad N, Romero DG, Gomez-Sanchez CE. Is aldosterone synthesized within the rat brain? *Am J Physiol Endocrinol Metab* 2005; **288**: E342–E346.
42 Geerling JC, Loewy AD. Aldosterone in the brain. *Am J Physiol Renal Physiol* 2009; **297**: F559–F576.
43 Funder JW. Mineralocorticoid receptors: distribution and activation. *Heart Fail Rev* 2005; **10**: 15–22.
44 Shibata S, Nagase M, Yoshida S, Kawarazaki W, Kurihara H, Tanaka H, Miyoshi J, Takai Y, Fujita T. Modification of mineralocorticoid receptor function by Rac1 GTPase: implication in proteinuric kidney disease. *Nat Med* 2008; **14**: 1370–1376.
45 Duc C, Farman N, Canessa CM, Bonvalet JP, Rossier BC. Cell-specific expression of epithelial sodium channel alpha, beta, and gamma subunits in aldosterone-responsive epithelia from the rat: localization by in situ hybridization and immunocytochemistry. *J Cell Biol* 1994; **127**: 1907–1921.
46 Nakagaki T, Hirooka Y, Matsukawa R, Nishihara M, Nakano M, Ito K, Hoka S, Sunagawa K. Activation of mineralocorticoid receptors in the rostral ventrolateral medulla is involved in hypertensive mechanisms in stroke-prone spontaneously hypertensive rats. *Hypertens Res* 2012; **35**: 470–476.
47 Kumar NN, Goodchild AK, Li Q, Pilowsky PM. An aldosterone-related system in the ventrolateral medulla oblongata of spontaneously hypertensive and wistar-kyoto rats. *Clin Exp Pharmacol Physiol* 2006; **33**: 71–75.
48 Amin MS, Reza E, Wang H, Leenen FH. Sodium transport in the choroid plexus and salt-sensitive hypertension. *Hypertension* 2009; **54**: 860–867.
49 Kolla V, Litwack G. Transcriptional regulation of the human Na/K ATPase via the human mineralocorticoid receptor. *Mol Cell Biochem* 2000; **204**: 35–40.

Original Article

Pitavastatin-Incorporated Nanoparticle-Eluting Stents Attenuate In-Stent Stenosis without Delayed Endothelial Healing Effects in a Porcine Coronary Artery Model

Noriaki Tsukie[1], Kaku Nakano[1], Tetsuya Matoba[1], Seigo Masuda[1], Eiko Iwata[1], Miho Miyagawa[1], Gang Zhao[3], Wei Meng[3], Junji Kishimoto[2], Kenji Sunagawa[1] and Kensuke Egashira[1]

[1]Department of Cardiovascular Medicine, Graduate School of Medical Sciences, Kyushu University, Fukuoka, Japan
[2]Digital Medicine Initiative, Graduate School of Medical Sciences, Kyushu University, Fukuoka, Japan
[3]Department of Cardiovascular Medicine, 6th People's Hospital, Shanghai Jiatong University, Shanghai, China

Aim: The use of currently marketed drug-eluting stents presents safety concerns including increased late thrombosis, which is thought to result mainly from delayed endothelial healing effects (impaired re-endothelialization resulting in abnormal inflammation and fibrin deposition). We recently developed a bioabsorbable polymeric nanoparticle (NP)-eluting stent using a novel cationic electrodeposition technology. Statins are known to inhibit the proliferation of vascular smooth muscle cells (VSMC) and to promote vascular healing. We therefore hypothesized that statin-incorporated NP-eluting stents would attenuate in-stent stenosis without delayed endothelial healing effects.
Methods: Among six marketed statins, pitavastatin (Pitava) was found to have the most potent effects on VSMC proliferation and endothelial regeneration *in vitro*. We thus formulated a Pitava-NP-eluting stent (20 μg Pitava per stent).
Results: In a pig coronary artery model, Pitava-NP-eluting stents attenuated in-stent stenosis as effectively as polymer-coated sirolimus-eluting stents (SES). At SES sites, delayed endothelial healing effects were noted, whereas no such effects were observed in Pitava-NP-eluting stent sites.
Conclusion: Pitava-NP-eluting stents attenuated in-stent stenosis as effectively as SES without the delayed endothelial healing effects of SES in a porcine coronary artery model. This nanotechnology platform could be developed into a safer and more effective device in the future.

J Atheroscler Thromb, 2013; 20:32-45.

Key words; Statin, Nanotechnology, Drug delivery system, Signal transduction

Introduction

Increased risk of late in-stent thrombosis resulting in acute coronary syndrome (unstable angina, acute myocardial infarction and death) after the use of drug-eluting stent (DES) devices has become a major safety concern[1-3]. These adverse effects are thought to result mainly from the anti-healing effects of the drugs (sirolimus and paclitaxel) on endothelial cells, leading to impaired re-endothelialization, excessive inflammation, proliferation and fibrin deposition[4-6]. These "anti-healing" drugs are used in most newer generation DESs, leading to continued safety concerns; therefore, the cellular and/or molecular targeting of both VSMC proliferation and re-endothelialization is an essential requirement for the development of more efficient and safer DESs. The use of an anti-healing approach that accelerates re-endothelialization, protects against thrombosis and decreases restenosis is warranted. Comparator analysis of endothelial cell coverage in four marketed polymeric DESs in rabbits has demonstrated a disparity in arterial healing; notably, all DESs examined showed a lack of endothelial anticoagulant function, independent of endothelial coverage[7].

Address for correspondence: Kensuke Egashira, Department of Cardiovascular Medicine, Graduate School of Medical Science, Kyushu University, 3-1-1, Maidashi, Higashi-ku, Fukuoka 812-8582, Japan
E-mail: egashira@cardiol.med.kyushu-u.ac.jp
Received: March 18, 2012
Accepted for publication: June 21, 2012